Dielectric properties of the $BaTi_{0.85}Zr_{0.15}O_3$ ceramics prepared by different techniques

Lavinia Petronela Curecheriu[1], Raluca Frunza[1] and Adelina Ianculescu[2]

[1]*Department of Solid State and Theoretical Physics, "Al. I. Cuza" University, Blv. Carol 11, Iasi, 700506, Romania*
[2]*Polytechnics University of Bucharest, 1-7 Gh. Polizu, P.O. Box 12-134, 011061 Bucharest, Romania*

Abstract

Three different processing routes, i.e. the classical solid state reaction technique the sol-precipitation method and the oxalate route, were employed for preparing $BaTi_{0.85}Zr_{0.15}O_3$ ceramics. The dielectric properties of these ceramics are comparatively analyzed. The obtained results show that the dielectric properties of these ceramics, even having the same composition, are highly sensitive to the preparation route, causing differences in the microstructures and in the local electrical inhomogeneity, thus, causing complicated dielectric relaxation phenomena.

Keywords: relaxor, chemical synthesis, dielectric characterization

I. Introduction

Barium titanate ($BaTiO_3$) – based ceramics are frequently used in applications like: multilayer ceramic capacitors (ceramics with specifications X7R, Y5V), materials in electronics for electrostriction and pulse generating devices, transducers, infrared detectors, tunable devices for microwave electronics etc., due to their high dielectric constant, good thermal shock resistance and dielectric reliability [1–3]. In addition, $BaTiO_3$ is an environment-friendly dielectric system with similar performances to Pb-based electroceramics. The properties of such materials can be tuned by doping, by forming solid solutions with other adequate systems and by controlling their microstructural characteristics (porosity level, grain size, secondary phases, core-shell structures, etc.).

In the last years, $BaZr_xTi_{1-x}O_3$ system became again attractive from the point of view of its characteristics related to the local polar properties [4], phase formation mechanism [5,6] and for the dielectric tunability properties in the view of microwave applications [7–9]. The dielectric data reported for $BaZr_xTi_{1-x}O_3$ ceramics suggest a normal ferroelectric behavior for compositions $0 \leq x \leq 0.15$, while for $0.15 \leq x \leq 0.42$ the material behaves as a ferroelectric relaxor. For $x > 0.50$, the system does not normally present any ferroelectric distortion. Therefore, the diffuseness of the ferroelectric – paraelectric phase transition increases with the Zr addition, x [10–12]. However, these limits are very sensitive to the preparation method, the presence of possible secondary phases and to the microstructural characteristics.

In the present work, the dielectrics properties of $BaZr_{0.15}Ti_{0.85}O_3$ (BZT) ceramics prepared by three methods (solid-state reaction, sol-precipitation and coprecipitation) techniques are comparatively investigated.

II. Experimental Procedure

Sample preparation

Three different processing routes, the classical solid state reaction technique, the sol-precipitation method and the oxalate route, noted as BZT1, BZT2, and BZT3, respectively, were used to analyse and compare the dielectric behaviour of the $BaTi_{0.85}Zr_{0.15}O_3$ ceramics.

For the classical solid state reaction method (BZT1), high-purity raw materials as $BaCO_3$ (Fluka), TiO_2 (Merck) and ZrO_2 (Merck) were weighed in appropriate proportions and homogenized with isopropyl alcohol in an agate mortar for 1 hour. The mixture was dried and then granulated using a 4 % PVA (polyvinyl alcohol) solution as binder agent, shaped by uniaxial pressing at 160 MPa into pellets of 20 mm diameter and ~ 3 mm thickness. The pre-sintering thermal treatment was carried

* Corresponding author: tel: +40 232 201 175, fax: +40 232 201 205,
e-mail: *lavinia_curecheriu@stoner.phys.uaic.ro*
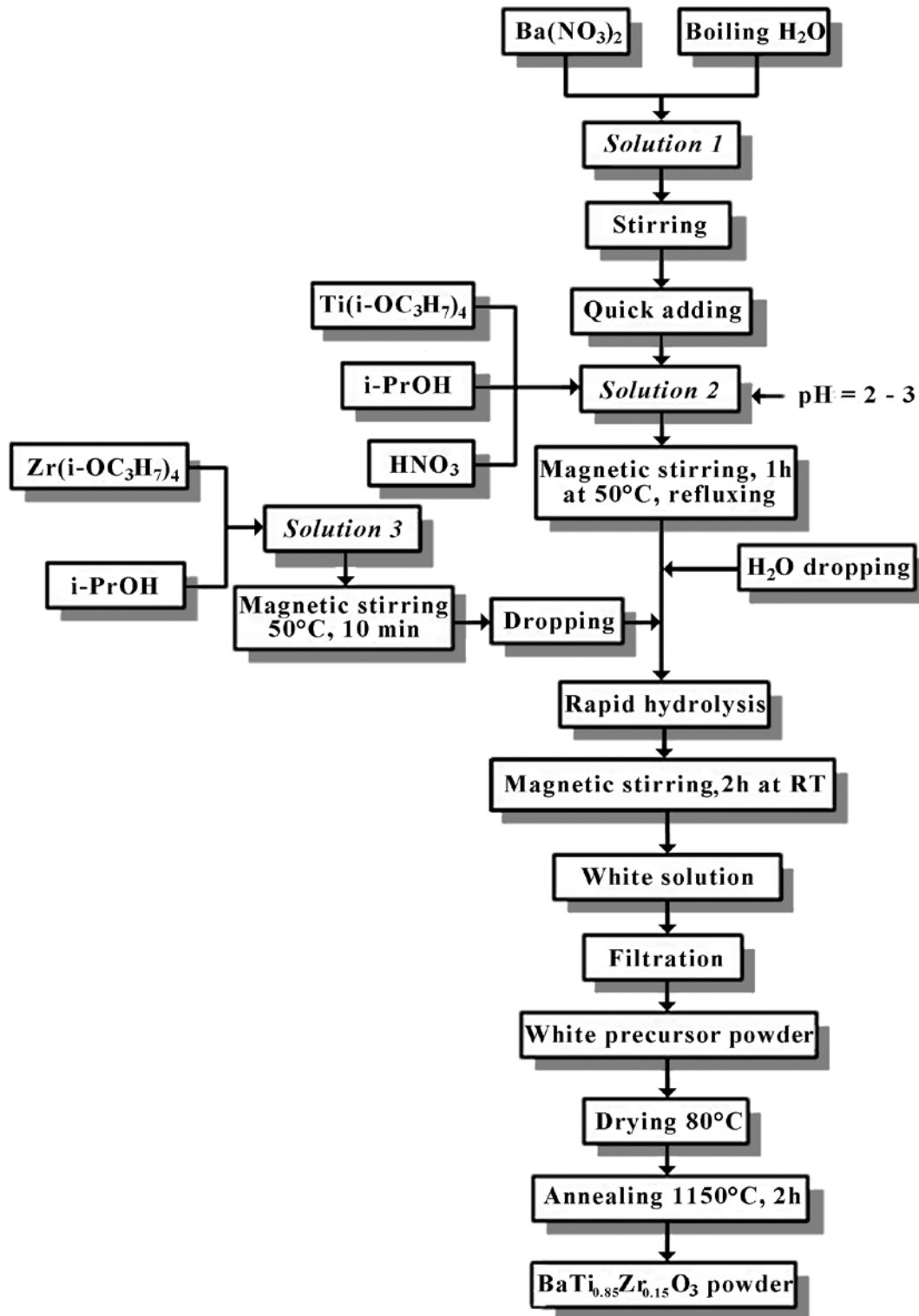
Figure 1. Flowchart for the synthesis of BaTi$_{0.85}$Zr$_{0.15}$O$_3$ powder by sol-precipitation method

out in air, at 1150°C, with 3 hours plateau. The samples were slowly cooled, then ground, pressed again into pellets of 10 mm diameter and 1–2 mm thickness and sintered in air, with a heating rate of 5°C/min, at 1300°C for 4 hours.

For the synthesis of the Ba(Ti,Zr)-precursor by sol-precipitation method (BZT2), Ba(NO$_3$)$_2$ (Merck),

Ti(i-OC$_3$H$_7$)$_4$ (Merck) and Zr(OC$_3$H$_7$)$_4$ (Merck) were used as barium, titanium and zirconium sources, respectively. The synthesis procedure of the final BaTi$_{0.85}$Zr$_{0.15}$O$_3$ oxide powder is presented in Fig. 1.

Pure BaTi$_{0.85}$Zr$_{0.15}$O$_3$ powder (BZT3) was obtained after annealing at 850°C for 7 hours of the mixed Ba(Ti,Zr)O(C$_2$O$_4$)$_2$·xH$_2$O oxalate prepared by using tita-
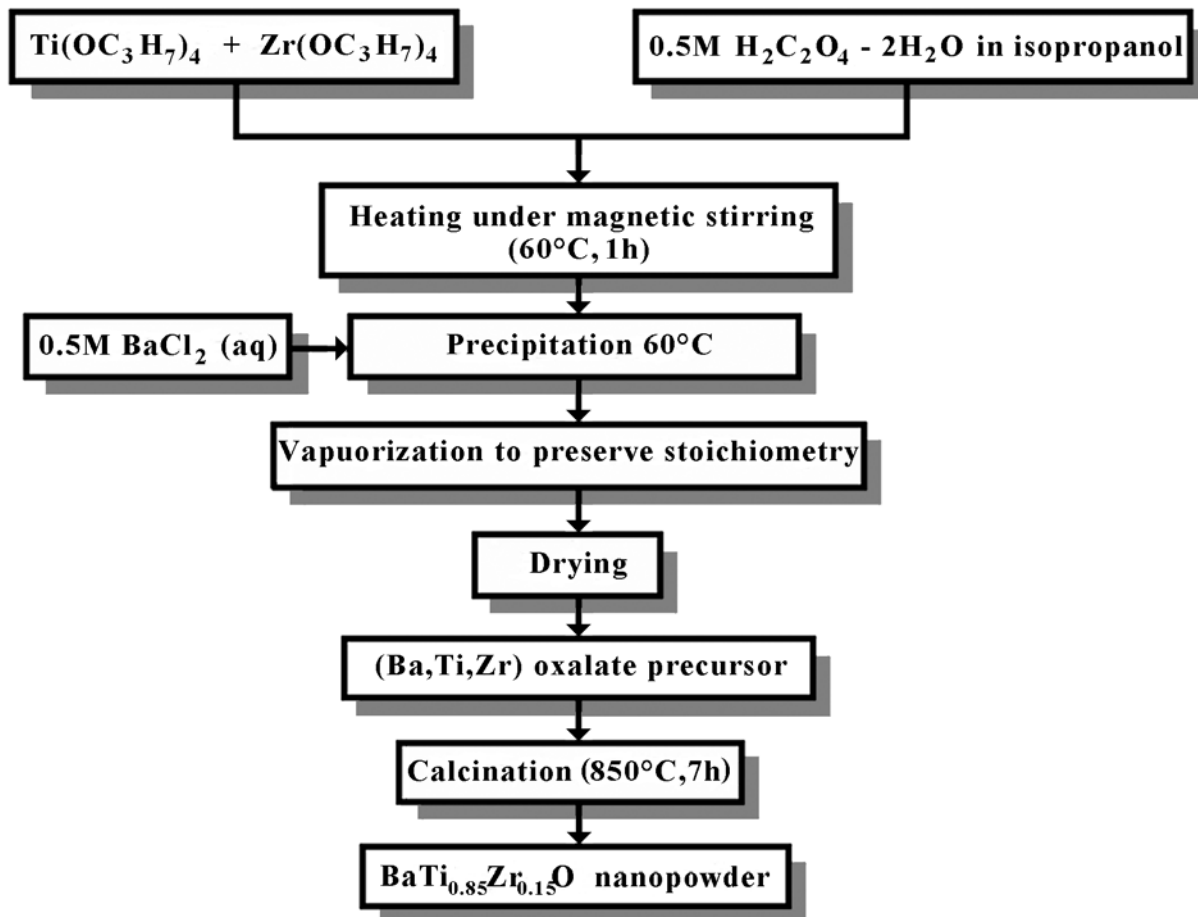
Figure 2. Flowchart for the synthesis of BaTi$_{0.85}$Zr$_{0.15}$O$_3$ powder by oxalate route

nium isopropoxid (Merck), zirconium propoxid (Merck) and barium chloride (Merck) as raw materials, oxalic acid (Merck) as chelating agent and isopropanol as solvent. The molar ratio was Ti(OC$_3$H$_7$)$_4$: Zr(OC$_3$H$_7$)$_4$: BaCl$_2$·2H$_2$O : H$_2$C$_2$O$_4$·2H$_2$O = 0.85 : 0.15 : 1 : 2. The synthesis flowchart is presented in Fig. 2.

Ceramics samples derived from the both powders synthesized by wet-chemical methods were obtained after pressing and sintering in the same conditions as the sample prepared by solid state reaction method (in air, at 1300°C for 4 hours).

Sample characterization

X-ray diffraction measurements, used to investigate the purity of the perovskite phase corresponding to the BZT solid solutions (powders and ceramics), were performed at the room temperature with a *SHIMADZU XRD 6000* diffractometer using Ni-filtered CuK$_\alpha$ radiation (λ = 1.5418 Å), with a scan step of 0.02° and a counting time of 1 s/step, for 2θ ranged between 20–120°. To estimate the structural characteristics of the powders and ceramics prepared in this work, a counting time of 10s/step, for 2θ ranged between 20–120° was used. The lattice constants calculation is based on the least squares procedure (LSP)

using the linear multiple regressions for several XRD lines, depending on the unit cell symmetry. A *HITACHI S2600N* scanning electron microscope coupled with EDX was used to analyze the ceramics microstructure and to check the chemical composition of the ceramic samples. The electrical measurements were performed on parallel-plate capacitor configuration, by applying Pd - Ag electrodes on the polished surfaces of the sintered ceramic disks. The complex impedance in the frequency domain of 20 to 2×10^6 Hz and for temperatures of 25–100°C was determined by using an Agilent E4980A impedance bridge.

III. Results and Discussion

The room temperature X-ray diffraction patterns of the samples sintered at 1300°C for 4 hours (Fig. 3) show single phase material, with well-developed diffraction peaks, mainly for the ceramics derived from the powders synthesized by wet-chemical methods. It is interesting to mention that the ceramics prepared by all the three methods already present a tetragonal structure, even if the values of the tetragonality are still low. The values of the structural parameters (unit cell parameters a and c, tetragonality a/c, unit cell volume V, crystallite

Table 1. Structural parameters of $BaTi_{0.85}Zr_{0.15}O_3$ ceramics sintered at 1300°C for 4 hours

Sample	BZT1	BZT2	BZT3
a (Å)	4.0284(32)	4.0337(17)	4.0224(40)
c (Å)	4.0420(53)	4.0517(27)	4.0428(67)
Tetragonalitz, c/a	1.0034(21)	1.0044(11)	1.0051(27)
Unit cell volume, V(Å)	65.59(19)	65.92(10)	65.41(24)
Crystallite size, (Å)	808(27)	621(12)	603(19)
Microstrains, Sx10³	0.97(4)	0.73(2)	1.02(4)

average size D and internal microstrains S) are summarized in Table 1.

The SEM image of the ceramic obtained by classical route using $BaCO_3$ and TiO_2 as raw materials shows an uniform microstructure, consisting of the small grains (~ 2 μm) with not well defined grain boundaries, as well as of a certain amount of inter-granular porosity (Fig. 4). The microstructure of the ceramics derived from powders synthesized by wet-chemical methods is also uniform, but unlike the sample obtained by solid state reaction, it consists of larger grains, with clearly marked grain boundaries (Figs. 5 and 6). Moreover, the sample BZT2 obtained from powders prepared by sol-precipitation method using barium nitrate ($Ba(NO_3)_2$), titanium iso-propoxid ($Ti(i\text{-}OC_3H_7)_4$) and zirconium propoxide ($Zr(OC_3H_7)_4$) as raw materials has a good sinterability, only a small amount of intergranular pores and an average grain size of ~ 6 μm (Fig. 5).

Slightly larger and better faceted grains, with an average size of ~ 9 μm, but also a higher inter-granular po-
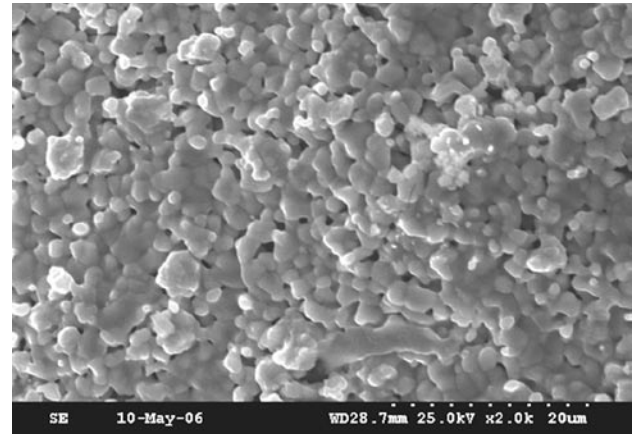
Figure 4. Surface SEM image of the polished ceramic sample (BZT1) obtained by solid state reaction route, after sintering at 1300°C/4h
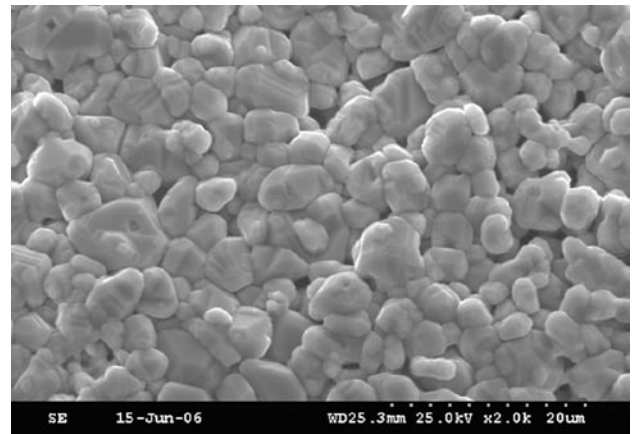
Figure 5. Surface SEM image of the polished ceramic sample (BZT2) derived from the powder prepared by sol-precipitation method (barium nitrate variant) after sintering at 1300°C/4h
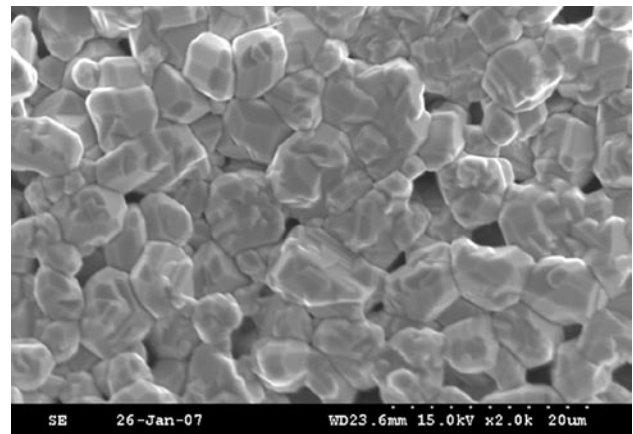
Figure 6. Surface SEM image of the polished ceramic sample (BZT3) derived from the powder prepared by oxalate route after sintering at 1300°C/4h
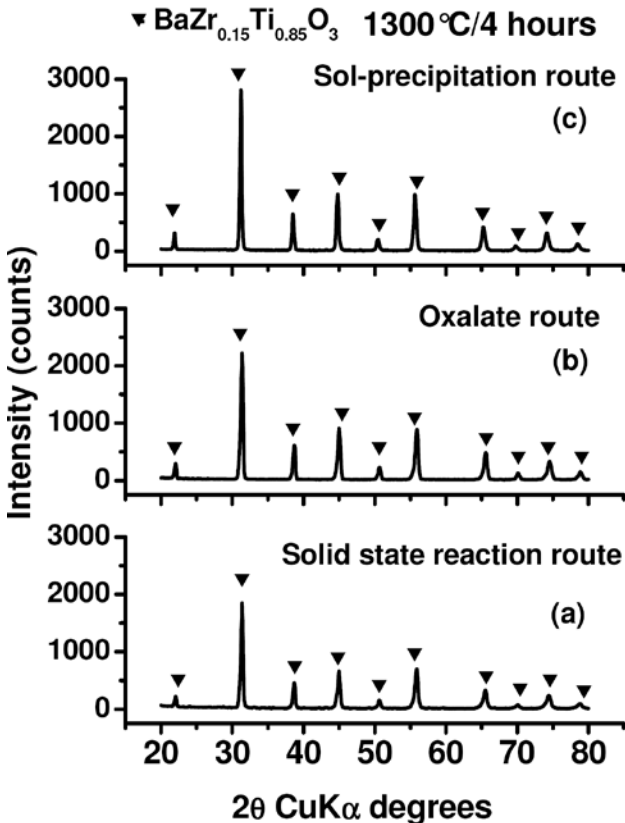
Figure 3. Room temperature X-ray diffraction patterns of $BaTi_{0.85}Zr_{0.15}O_3$ ceramic samples prepared by different methods
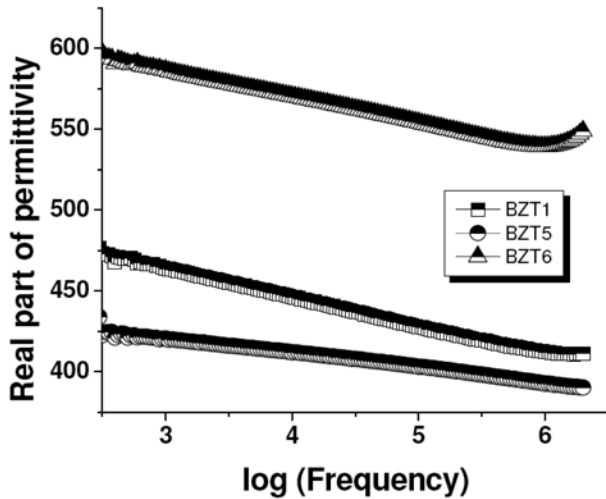
Figure 7. Frequency dependence of the real part of permittivity of BZT ceramics
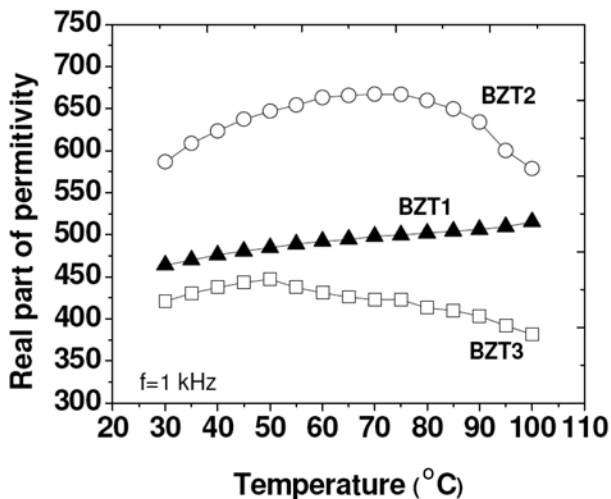
Figure 8. Temperature dependence of the real part of permittivity of BZT ceramics
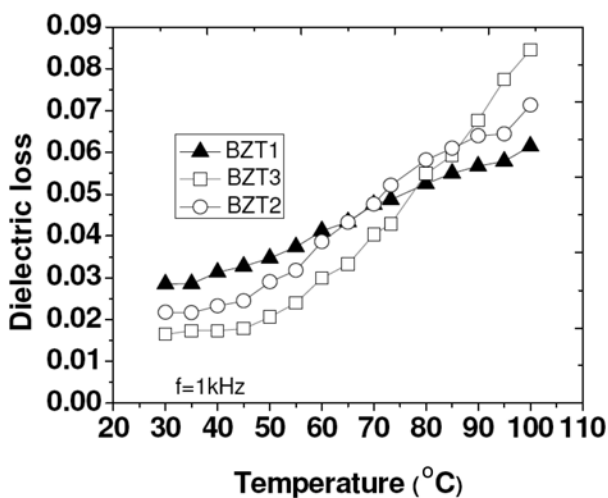
Figure 9. Temperature dependence of the dielectric losses in BZT ceramics

rosity was observed for the sample BZT3 derived from the powder synthesized by the oxalate route, using titanium isopropoxid, zirconium propoxid and barium chloride as raw materials (Fig. 6).

The permittivity vs. frequency of the BZT samples prepared by the three methods can be compared in Fig. 7. The samples have a low permittivity of around 400–600 at room temperature in the overall frequency range and presents a continuous fall with increasing frequency. Only the sample BZT2 shows an increasing permittivity at higher frequencies (2MHz) after this fall. The maximum available frequency in this experiment does not allow to decide if a relaxation mechanism possible related to domain walls motions is present in the BZT2 ceramic and why is not also visible in the behavior of the other samples.

The permittivity and dielectric losses vs. temperature of all samples at the 1 kHz are shown in Figs. 8 and 9. The ceramics have a rather low dielectric constant of about 450–650 and low dielectric losses below 9% for temperatures ranging from 20°C to 100°C. The dielectric losses at room temperature have values of 1.5–3% for all the BZT samples investigated here and an increase with the temperature rise, proving a thermally-activated loss mechanism (Fig. 9).

While the BZT2 ceramic shows a diffuse phase transition with a very broad maximum between 50 and 80°C, associated to the ferroelectric relaxor-paraelectric transition, an almost linear rise in the permittivity-temperature dependence seems to be characteristic for the sample BZT1, and a dependence with a maximum around 50°C associated to the ferroelectric-paraelectric transition for the BZT3 ceramic.

In order to understand if the phase transitions depend on the preparation methods, the dielectric properties as a function of temperature and frequency were carefully inspected for each sample. The dielectric properties of the BZT1, BZT2 and BZT3 samples at few frequencies in the range 1 kHz–2 MHz are presented in Fig. 10.

In the case of the BZT1 sample (Fig. 10a), the real part of permittivity increases with temperature and decreasing frequency. This increase of dielectric constant with temperature, particularly at high temperatures is most probably related to a degree of local inhomogeneity causing Maxwell-Wagner interface effects and has as a result the impossibility to detect the ferroelectric-paraelectric phase transition expected in the range of 50–80°C. Conversely, the BZT2 ceramic shows a well-defined broad peak (relaxor-ferroelectric) with a maximum located at around 65°C (Fig. 10b), while BZT3 (Fig. 10c) has a pronounced maximum at 50°C corresponding to the ferroelectric-paraelectric transition and the second anomaly around 85°C. This particular behavior is probably caused by a kind of well-segregated inhomogeneity within the ceramic sample, most probably due to compositional variations Zr/Ti inside the

grains, associated to variations of the local Curie temperatures. The large majority of ceramic grains/regions have an average Curie temperature at around 50°C and another smaller percentage at around 80°C. This hypothesis has to be further confirmed by SEM-EDX experiments aimed to detect the local Zr/Ti stoichiometry in the present ceramic samples.

Generally, the dielectric properties of electroceramics arise due to intra-grain, inter-grain and electrode effects. The motion of charges could take place by charge displacement, dipole reorientation, space charge formation, etc. In order to understand the electrical properties of a given sample, grain, grain boundary and electrode contributions must be separated. The intergrain boundaries in ceramics are defective regions, where deviations from oxygen stoichiometry and segregation of impurities, dopants or secondary phases could occur. Accordingly, it is expected that from the electrical point of view, the grain bulk and grain boundary regions should have different dielectric and conductive properties. In addition, the ceramic region in contact with electrodes might be "modified" with respect to the inner part of the bulk: different Fermi levels of the two materials in contact give rise to Schottky barriers, imperfect conductivity of the electrodes create a screening region changing the potential distribution in their neighborhood and metallic ions might diffuse into the ceramic creating a doped interface regions. In any of these situations, the dielectric and conductive properties at the contact electrode-ceramics might be different with respect to the rest of material. The complex impedance analysis has proved to be a very powerful tool for separating these contributions and it was used here to check if such inhomogeneities are visible in the complex impedance spectra of the present BZT ceramics.

The Cole-Cole plot at the temperatures of 40°C, 70°C and 100°C obtained for the BZT1 sample prepared by the solid state route (Fig. 11) clearly demonstrates the high degree of the electrical inhomogeneity of this sample. At 40°C, the complex permittivity plot shows three deconvoluted components which evolve in two components as the temperature increases. In the case of both BZT2 and BZT3 samples, only one component it was observed in the impedance plot. It is worth to mention that according to the temperature dependence of the permittivity for the BZT3 sample, shown in the Fig. 10c, a degree of inhomogeneity was also expected for the BZT3 ceramic. However, it seems that the compositional inhomogeneity (local Zr/Ti ratio) responsible with the local variation of the Curie temperatures does not cause multi-component Cole-Cole plot for this ceramic.

While the data for real homogeneous dielectrics actually fit an arc of a circle with the center below the real axis [13] and are described by an RC-equivalent circuit, for the polycrystalline ceramic material with
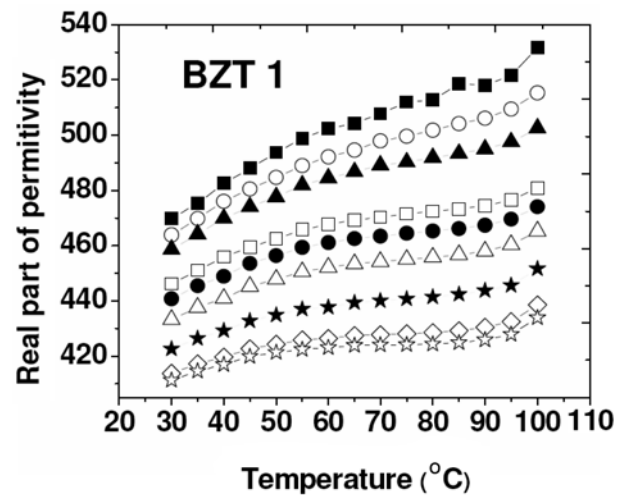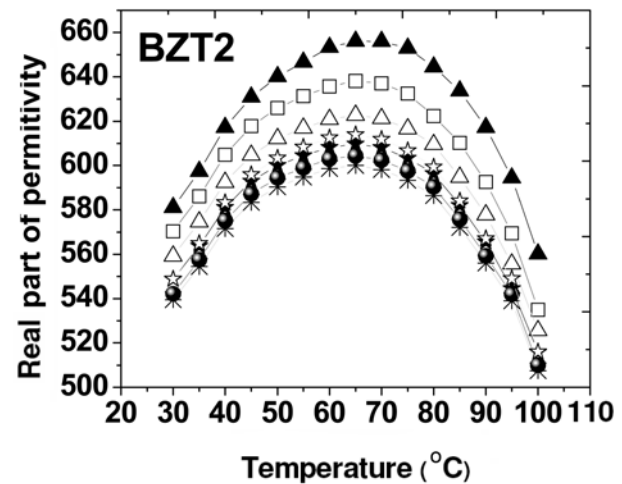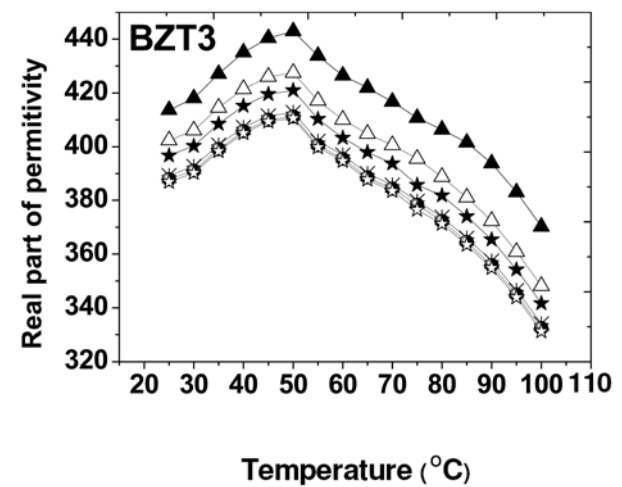
Figure 10. Permittivity vs. temperature at different frequencies: a) BZT1, b) BZT2, c) BZT3 (■ 500 Hz, ○ 1 kHz, ▲ 2 kHz, □ 10 kHz, ● 20 kHz, △ 50 kHz, ★ 200 kHz, ◇ 750 kHz, ✳ 1 MHz, ⬤ 1.5 MHz and ☆ 2 MHz)

electrodes, a more complex model is appropriate, in which different groups of RC-circuits describe: (a) the ceramic grain (high frequency, close to the axis origin of the Cole-Cole plot), (b) the ceramic grain boundaries (in the middle part of the Cole-Cole plot), (c) the electrode-ceramic interfaces (for low frequencies, at high values of ε') (Fig.12).
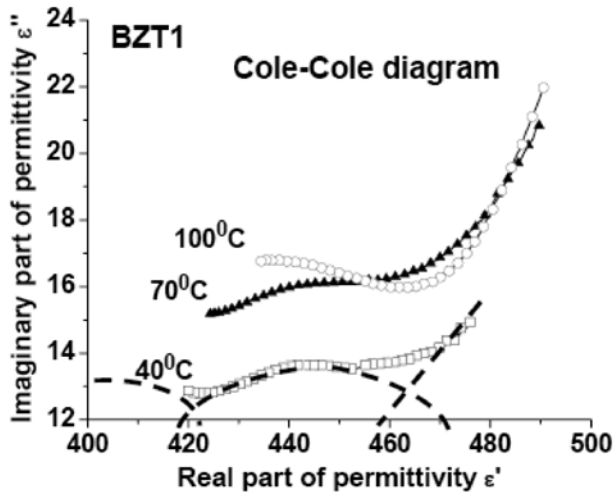
Figure 11. Cole-Cole plot at different temperatures obtained for the BZT1 ceramic showing a few impedance components

The second component is missing in single-crystals and is enhanced in fine grained ceramics, due to the large number of grain boundaries in such structures. Dependent on their electrical properties (values of the equivalent impedance of the regions), often the contributions are convoluted and in such case their separation is very difficult. In the case of the BZT1 sample, such components are observed. In addition, in the solid solutions, local composition inhomogeneity gives rise to possible local variation of the polarization re-
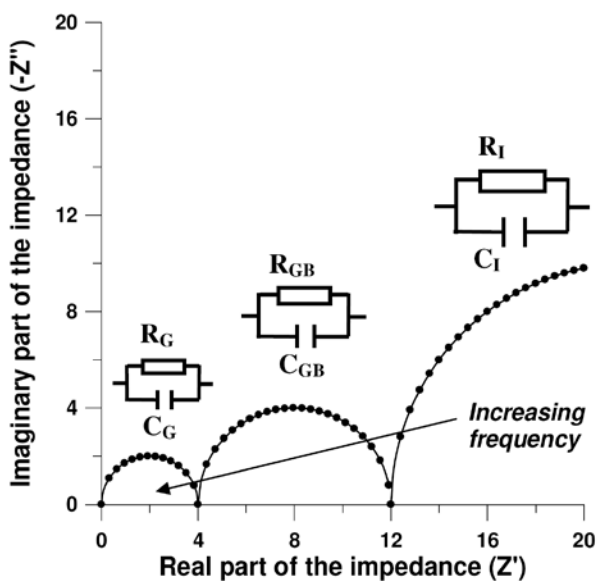
Figure 12. Model using for explication of a real electroded ceramic containing three distinct contributions: ceramic grain (R_G, C_G), ceramic grain boundaries (R_{GB}, C_{GB}) and electrode-ceramic interfaces (R_I, C_I)

sulting in uncompensated bounded charges in the volume of the sample. They normally produce an extrinsic (not related to the ferroelectric lattice) electrostatic polarization called space charge or Maxwell-Wagner effect [14]. All BZT solid solutions and particularly the BZT1 show such a behaviour, which is manifested by a frequency-dependence of the dielectric constant in the paraelectric state together with an anomalous increase of the dielectric losses, mainly at high temperatures.

The high porosity and fine grain size are also contributing to the complexity of the dielectric response. By considering the possible defects in the perovskite ceramics, it seems that the oxygen vacancies are the most probably responsible for the observed effect [15]. Their concentration might be different in the grain and grain boundaries as a result of processing, causing multiple components in the Cole-Cole plot.

IV. Conclusions

Three different methods were used to prepare the BZT ceramics: solid state, sol-precipitation and coprecipitation. The samples were sintered in the same conditions, at 1300°C for 4h.

The results obtained for the present samples show that the dielectric properties of the BZT ceramics are highly sensitive to the local electrical inhomogeneity, causing complicated dielectric relaxation phenomena. Further studies aimed to improve the microstructure, to increase the grain size and density, the local homogeneity, as well as the oxygen stoichiometry are expected to result in better dielectric responses in such BZT ceramics.

References

1. M.E. Lines, A.M. Glass, *Principles and applications of ferroelectrics and related materials*, Clarendon Press, Oxford, 1977.
2. Y. Xu, *Ferroelectric materials and their applicati-ons*, North Holland Elsevier Sci. Publ., Amsterdam, 1991.
3. U. Böttger, *Dielectric properties of polar oxides, in Polar oxides: properties, characterization and imaging*, ed. R. Waser, U. Böttger, S. Tiedke, Wiley-VCH Verlag GmbH&Co. KGaA, Weinheim, 2005.
4. R. Farhi, M. El Marssi, A. Simon, J. Ravez, "Raman and dielectric study of ferroelectric Ba(Ti$_{1-x}$Zr$_x$)O$_3$ ceramics", *Eur. Phys. Journal*, **B 9** (1999), 599.
5. K. Aliouane, A. Guehria-Laidoudi, A. Simon, J. Ravez, "Study of new relaxor materials in BaTiO$_3$-BaZrO$_3$-La$_{2/3}$TiO$_3$ system", *Solid State Ionics*, **7** (2005) 1324.
6. J. Bera, S.K. Rout, "On the formation mechanism of BaTiO$_3$–BaZrO$_3$ solid solution through solid-oxide reaction", *Mater. Lett.*, **59** (2005) 135.

7. U. Weber, G. Greuel, U. Boettger, S. Weber, D. Hennings, R. Waser, "Dielectric properties of Ba(Zr,Ti)O$_3$-based ferroelectrics for capacitor applications", *J. Am. Ceram. Soc.*, **84** (2001) 759.

8. Z. Yu, C. Ang, R. Guo, A.S. Bhalla, "Dielectric properties and high tunability of Ba(Ti$_{0.7}$Zr$_{0.3}$)O$_3$ ceramics under dc electric field", *Appl. Phys. Lett.*, **81** (2002) 1285.

9. Q. Feng, C.J. McConville, D.D. Edwards, **"**Dielectric properties and microstructures of Ba(Ti,Zr)O$_3$ multilayer ceramic capacitors with Ni electrodes", *J. Am. Ceram. Soc.*, **88** (2005) 1455.

10. D. Hennings, H. Schell, "Diffuse ferroelectric phase transitions in Ba(Ti$_{1-y}$Zr$_y$)O$_3$ ceramics"*, J. Am. Ceram. Soc.*, **65** (1982) 539.

11. S. M. Neirman, "The Curie point temperature of Ba(Ti$_{1-x}$Zr$_x$)O$_3$ solid solutions", *J. Mater. Sci.*, **23** (1988) 3973.

12. J. Ravez, A. Simon, **"**Temperature and frequency dielectric response of ferroelectric ceramics with composition Ba(Ti$_{1-x}$Zr$_x$)O$_3$", *J. Eur. Solid State Inorg. Chem.*, **34** (1997) 1199.

13. A.K. Jonscher, *Dielectric Relaxation in Solids*, London, Chelsea Dielectric Press (1983).

14. Z. Yu, C. Ang, "Maxwell-Wagner polarization in ceramic composites BaTiO$_3$–(Ni$_{0.3}$Zn$_{0.7}$)Fe$_{2.1}$O$_4$", *J. Appl. Phys.*, **91** (2002) 794.

15. Z. Yu, C. Ang, R. Guo, A.S. Bhalla*,* "Ferroelectric-relaxor behavior of Ba(Ti$_{0.7}$Zr$_{0.3}$)O$_3$ ceramics", *J. Appl. Phys.*, **92** (2002) 2655.